Environmental noise reduction for holonomic quantum gates

Daniele Parodi,[1,2] Maura Sassetti,[1,3] Paolo Solinas,[4] Nino Zanghì[1,2]

[1] *Dipartimento di Fisica, Università di Genova*
[2] *Istituto Nazionale di Fisica Nucleare (Sezione di Genova),*
[3] *INFM-CNR Lamia*
Via Dodecaneso 33, 16146 Genova, Italy
[4] *Laboratoire de Physique Théorique de la Matière Condensée,*
Université Pierre et Marie Curie,
Place Jussieu, 75252 Paris Cedex 05, France
(Dated: May 15, 2019)

We study the performance of holonomic quantum gates, driven by lasers, under the effect of a dissipative environment modeled as a thermal bath of oscillators. We show how to enhance the performance of the gates by suitable choice of the loop in the manifold of the controllable parameters of the laser. For a simplified, albeit realistic model, we find the surprising result that for a long time evolution the performance of the gate (properly estimated in terms of average fidelity) increases. On the basis of this result, we compare holonomic gates with the so-called STIRAP gates.

I. INTRODUCTION

The major challenge for quantum computation is posed by the fact that generically quantum states are very delicate objects quite difficult to control with the required accuracy—typically, by means of external driving fields, e.g., a laser. The interaction with the many degree of freedom of the environment causes decoherence; moreover, errors in processing the information may lead to a wrong output state.

Among the approaches aiming at overcoming these difficulties are noteworthy those for which the quantum gate depends very weakly on the details of the dynamics, in particular, the holonomic quantum computation (HQC) [1] and the so-called STIRAP [2, 3, 4]. In the latter, the gate operator is obtained acting on the phase difference of the driving lasers during the evolution, while in the former the same goal is achieved by exploiting the non-commutative analogue of the Berry phase collected by a quantum state during a cyclic evolution. Concrete proposals have been put forward, for both Abelian [5, 6] and non-Abelian holonomies [7, 8, 9, 10, 11, 12]. The main advantage of the HQC is the robustness against noise deriving from a imperfect control of the driving fields [13, 14, 15, 16, 17, 18, 19].

In a recent paper [20] we have shown that the disturbance of the environment on holonomic gates can be suppressed and the performance of the gate optimized for particular environments (purely super-ohmic thermal bath). In the present paper we consider a different sort of optimization, which is independent of the particular nature of the environment.

By exploiting the full geometrical structure of HQC, we show how the performance of a holonomic gate can be enhanced by suitable choice of the loop in the manifold of the parameters of the external driving field: by choosing the *optimal loop* which minimizes the "error" (properly estimated in terms of average fidelity loss). Our result is based on the observation that there are different loops in the parameter manifold producing the same gate and, since decoherence and dissipation crucially depend on the dynamics, it is possible to drive the system over trajectories which are less perturbed by the noise. For a simplified, albeit realistic model, we find the surprising result that the error decreases linearly as the gating time increases. Thus the disturbance of the environment can be drastically reduced. On the basis of this result, we compare holonomic gates with the STIRAP gates.

In Section II the model is introduced and the explicit expression of the error is derived. In Section III we find the optimal loop, calculate the error, make a comparison with other approaches, and briefly sketch how to treat a different coupling with the environment.

II. MODEL

The physical model is given by three degenerate (or quasi-degenerate) states, $|+\rangle$, $|-\rangle$, and $|0\rangle$, optically connected to another state $|G\rangle$. The system is driven by lasers with different frequencies and polarizations, acting selectively on the degenerate states. This model describes various quantum systems interacting with a laser radiation, ranging from semiconductor quantum dots, such as excitons [12] and spin-degenerate electron states [3], to trapped ions [8] or neutral atoms [7].

The (approximate) Hamiltonian modeling the effect of the laser on the system is (for simplicity, $\hbar = 1$) [8, 12]

$$H_0(t) = \sum_{j=+,-,0} \left[\epsilon|j\rangle\langle j| + (e^{-i\epsilon t}\Omega_j(t)|j\rangle\langle G| + h.c) \right], \quad (1)$$

where $\Omega_j(t)$ are the time dependent Rabi frequencies depending on controllable parameters, such as the phase and intensity of the lasers, and ϵ is the energy of the degenerate electron states. The Rabi frequencies are

modulated within the adiabatic time t_{ad}, (which coincides with the gating time), to produce a loop in the parameter space and thereby realize the periodic condition $H_0(t_{ad}) = H_0(0)$.

The Hamiltonian (1) has four time dependent eigenstates: two eigenstates $|E_i(t)\rangle$, $i = 1, 2$, called *bright states*, and two eigenstates $|E_i(t)\rangle$, $i = 3, 4$, called *dark states*. The two dark states have degenerate eigenvalue ϵ and the two bright states have time dependent energies $\lambda_\pm(t) = (\epsilon \pm \sqrt{\epsilon^2 + 4\Omega^2(t)})/2$ with $\Omega^2(t) = \sum_{i=\pm,0} |\Omega_i(t)|^2$ [21].

The evolution of the state is generated by

$$U_t = \mathrm{T}e^{-i\int_0^t dt' H_0(t')}, \qquad (2)$$

where T is the time-ordered operator. In the adiabatic approximation, the evolution of the state takes place in the degenerate subspace generated by $|+\rangle$, $|-\rangle$ and $|0\rangle$. This approximation allows to separate the dynamic contribution and the geometric contribution from the evolution operator. Expanding U_t in the basis of instantaneous eigenstates of $H_0(t)$ (the bright and dark states), in the adiabatic approximation, we have

$$U_t \cong \sum_j e^{-i\int_0^t E_j(t')dt'}|E_j(t)\rangle\langle E_j(t)| \, \mathcal{U}_t, \qquad (3)$$

where

$$\mathcal{U}_t = \mathrm{T}e^{\int_0^t d\tau V(\tau)}, \qquad (4)$$

here V is the operator with matrix elements $V_{ij}(t) = \langle E_i(t)|\partial_t|E_j(t)\rangle$. The unitary operator $\mathcal{U}_t$ plays the role of time dependent holonomic operator and is the fundamental ingredient for realizing complex geometric transformation whereas $\sum_j e^{-i\int_0^t E_j(t')dt'}|E_j(t)\rangle\langle E_j(t)|$ is the dynamic contribution.

Consider $\mathcal{U}_t$ for a closed loop, i.e. for $t = t_{ad}$,

$$\mathcal{U} = \mathcal{U}_{t_{ad}}. \qquad (5)$$

If the initial state $|\psi_0\rangle$ is a superposition of $|+\rangle$ and $|-\rangle$, then $\mathcal{U}|\psi_0\rangle$ is still a superposition of the same vectors (in general, with different coefficients)[12]. Thus the space spanned by $|+\rangle$ and $|-\rangle$ can be regarded as the "logical space" on which the "logical operator" $\mathcal{U}$ acts as a "quantum gate" operator. Note that for $t < t_{ad}$, $\mathcal{U}_t|\psi_0\rangle$ has, in general, also a component along $|0\rangle$. However, as it is easy to show [21], at any instant $t < t_{ad}$, $\mathcal{U}_t|\psi_0\rangle$ can be expanded in the two dimensional space spanned by the dark states $|E_3(t)\rangle$ and $|E_4(t)\rangle$. It is important to observe that $\mathcal{U}$ depends only on global geometric features of the path in the parameter manifold and not on the details of the dynamical evolution [1, 12].

To construct a complete set of holonomic quantum gates, it is sufficient to restrict the Rabi frequencies $\Omega_j(t)$ in such a way that the norm Ω of the vector $\vec{\Omega} = (\Omega_0(t), \Omega_+(t), \Omega_-(t))$ is time independent and the vector lies on a real three dimensional sphere [8, 12].

We parametrize the evolution on this sphere as $\Omega_+(t) = \sin\theta(t)\cos\phi(t)$, $\Omega_-(t) = \sin\theta(t)\sin\phi(t)$ and $\Omega_0(t) = \cos\theta(t)$ with fixed initial (and final) point in $\theta(0) = 0$, the *north pole* By straightforward calculation we obtain the analytical expression for $V(t)$ in equation (4), $V(t) = i\sigma_y cos[\theta(t)]\dot\phi(t)$, where σ_y is the usual Pauli matrix written in the basis of dark states. Thus, the operator (4) becomes $\mathcal{U}_t = \cos[a(t)] - i\sigma_y\sin[a(t)]$, here $a(t) = \int_0^t d\tau\dot\phi(\tau)\cos\theta(\tau)$. Accordingly, the logical operator $\mathcal{U}$ (5) is

$$\mathcal{U} = \cos a - i\sigma_y\sin a \qquad (6)$$

where

$$a = a(t_{ad}) = \int_0^{t_{ad}} d\tau\dot\phi(\tau)\cos\theta(\tau) \qquad (7)$$

is the solid angle spanned on the sphere during the evolution. Note that the are many paths on the sphere which generate the same logical operator $\mathcal{U}$, and span the same solid angle a.

In a previous work we have studied how interaction with the environment disturbs the logical operator $\mathcal{U}$ [20]. The goal of the present paper is to analyze whether and how such a disturbance can be minimized for a given $\mathcal{U}$. To this end, we model the environment as a thermal bath of harmonic oscillators with linear coupling between system and environment [22]. The total Hamiltonian is then

$$H = H_0(t) + \sum_{\alpha=1}^N (\frac{p_\alpha^2}{2m_\alpha} + \frac{1}{2}m_\alpha\omega_\alpha^2 x_\alpha^2 + c_\alpha x_\alpha A), \quad (8)$$

where A is the system interaction operator called, from now, *noise operator*.

We now consider the time evolution of the reduced density matrix of the system, determined by the Hamiltonian (8). We rely on the standard methods of the "master equation approach", with the environment treated in the Born approximation and assumed to be at each time in its own thermal equilibrium state at temperature T. This allow to include the effect of the environment in the correlation function ($k_B = 1$)

$$g(\tau) = \int_0^\infty J(\omega)\big[\coth(\frac{\omega}{2T})\cos(\omega\tau) - i\sin(\omega\tau)\big]d\omega. \quad (9)$$

Here the spectral density is

$$J(\omega) = \frac{\pi}{2}\sum_{\alpha=1}^N \frac{c_\alpha^2}{m_\alpha\omega_\alpha}\delta(\omega - \omega_\alpha), \qquad (10)$$

at the low frequencies regimes, is proportional to ω^s, with $s \geq 0$, i.e. $s = 1$ describes a Ohmic environments, typical of baths of conductions electron, $s = 3$ describes a super-Ohmic environments, typical of baths of phonons [20, 23]. The asymptotic decay of the real part of $g(\tau)$ defines the characteristic memory time of the environment.

Denoting with $\tilde{\rho}(t)$ the time evolution of the reduced density matrix of the system in the interaction picture, e.g., $\tilde{\rho}(t) = U_t^\dagger \rho U_t$, one has [23]

$$
\begin{aligned}
\tilde{\rho}(t_{ad}) = \ & \rho(0) + \\
& - i \int_0^{t_{ad}} dt \int_0^t d\tau \{ g(\tau)[\tilde{A}\tilde{A}'\tilde{\rho}(t-\tau) - \tilde{A}'\tilde{\rho}(t-\tau)\tilde{A}] \\
& + g(-\tau)[\tilde{\rho}(t-\tau)\tilde{A}'\tilde{A} - \tilde{A}\tilde{\rho}(t-\tau)\tilde{A}'].
\end{aligned} \tag{11}
$$

Here $\tilde{A}$ and $\tilde{A}'$ stand for $\tilde{A}(t)$ and $\tilde{A}(t-\tau)$, with the superscript tilde denoting the time evolution in the interaction picture.

In quantum information the quality of a gate is usually evaluated by the fidelity $\mathcal{F}$, which measures the closeness between the unperturbed state and the final state,

$$
\mathcal{F} = \langle \psi_0(0)|\mathcal{U}^\dagger \rho(t_{ad})\mathcal{U}|\psi_0(0))\rangle. \tag{12}
$$

where $|\psi_0(0)\rangle$ is the initial state, and $\rho(t_{ad}) = \mathcal{U}\tilde{\rho}(t_{ad})\mathcal{U}^\dagger$ is the reduced density matrix in the Schroedinger picture starting from the initial condition $\rho(0) = |\psi_0(0)\rangle\langle\psi_0(0)|$. The average error is defined as the average fidelity loss, i.e.,

$$
\delta = <1 - \mathcal{F}> = 1 - <\langle \psi_0(0)|\tilde{\rho}(t_{ad})|\psi_0(0)\rangle>, \tag{13}
$$

where $< \cdots >$ denotes averaging with respect to the uniform distribution over the initial state $|\psi_0(0)\rangle$.

The RHS of Eq. (13) can be computed by the following steps:
1) solving Eq. (11) in *strictly second order approximation*; this approximation corresponds to replace $\tilde{\rho}(t-\tau)$ with $\rho(0)$;
2) using the adiabatic approximation $U(t-\tau, t) \approx \exp(i\tau H_0(t))$;
3) expanding the scalar product in Eq. (13) with respect to a complete orthonormal basis $\{|\varphi_n(t)\rangle\}$, $n = 1, 2, 3$, orthogonal to $|\psi_0(t)\rangle$. In this way, one obtains

$$
\delta = <\sum_{n=1}^3 \int_0^{t_{ad}} dt \, G(t)|\langle \psi_0(t)|A|\varphi_n(t)\rangle|^2>, \tag{14}
$$

where

$$
G(t) = \int_0^t d\tau \left[Re(g(\tau))\cos(\omega_{0n}t) + Im(g(\tau))\sin(\omega_{0n}t) \right]. \tag{15}
$$

Here, $\omega_{0n} = \omega_0 - \omega_n$ are the energy differences associated to the transition $\psi_0 \leftrightarrow \phi_n$, with $\omega_0 = \epsilon$, $\omega_1 = \lambda_+$, $\omega_2 = \lambda_-$ and $\omega_3 = \epsilon$.

The interaction between system and environment is expressed by the noise operator A in Eq (8). We shall now make the assumption that $A = diag\{0, 0, 0, 1\}$ in the $|G\rangle$, $|\pm\rangle$ and $|0\rangle$ basis. In this case the transition between degenerate states are forbidden but the noise breaks their degeneracy shifting one of them. In spite of its simple form, this A is nevertheless a realistic noise operator for physical semiconductor systems [4].

III. MINIMIZING THE ERROR

The problem can be stated in the following way: given the noise operator A and the logical operator $\mathcal{U}$, find a path on the parameter space (the surface of the sphere, described above) which minimizes the error δ.

The total error δ, given by the Eq. (14), can be decomposed as

$$
\delta = \delta_{tr} + \delta_{pd}, \tag{16}
$$

where the transition error, δ_{tr}, is the contribution to the sum of the non-degenerate states ($\omega_{0n} \neq 0$) and the pure dephasing error δ_{pd} is the contribution of the degenerate states ($\omega_{0n} = 0$). Thus

$$
\begin{aligned}
\delta_{pd} = \ & \frac{\pi}{8} \int_0^{t_{ad}} dt \int_0^\infty d\omega \frac{J(\omega)}{\omega} \coth(\frac{\omega}{2T}) \\
& \sin(\omega t)(1 + \frac{1}{2}\sin^2 2a(t))\sin^4\theta(t)
\end{aligned} \tag{17}
$$

and

$$
\delta_{tr} = \sum_{n=+,-} \frac{1}{8\sqrt{1 + [(\lambda_n - \epsilon)/\Omega]^2}} \Gamma_{0n} \int_0^{t_{ad}} \sin^2 2\theta(t) dt, \tag{18}
$$

where

$$
\Gamma_{0n} = J(|\omega_{0n}|)\left[\coth\left(\frac{|\omega_{0n}|}{2T} \right) - \text{sign}(\omega_{0n}) \right] \tag{19}
$$

correspond to the transition rates calculated by standard Fermi Golden Rules, supposing, as usual, $G(t) \approx G(\infty)$ for $g(\tau)$ strongly peaked around $\tau = 0$. In the following we define for simplicity

$$
K = \sum_{n=+,-} \frac{1}{8\sqrt{1 + [(\lambda_n - \epsilon)/\Omega]^2}} \Gamma_{0n}.
$$

Since we are interested at long time evolution, we start discussing the transition error which dominates in this regime [4, 24].

A. Transition rate

As explained in Section II, the holonomic paths are closed curves on the surface of the sphere which start from the north pole. It turns out that the curve minimizing δ_{tr} can be found among the loops which are composed by a simple sequence of three paths (see Appendix A): evolution along a *meridian* ($\phi = const$), evolution along a *parallel* ($\theta = const$) and a final evolution along a *meridian* to come back to the north pole.

The error δ_{tr} in (18), depends on a given by Eq. (7), θ_M (the maximum angle spanned during the evolution along the meridian), $\Delta\phi$ (the angle spanned along the parallel) and angular velocity v. We allow $\Delta\phi \geq 2\pi$
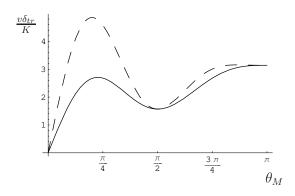
FIG. 1: The error δ_{tr} versus θ_M for two different a values: $a = \pi/2$ (dashed line) and $a = \pi/4$ (full line) correspond to NOT and Hadamard gate respectively.

which corresponds to cover more than one loop along the parallel. The velocity along the parallel is $v(t) = \dot{\phi}(t) \sin \theta$ and that along the meridian is $v(t) = \dot{\theta}(t)$. In the following we assume that v is constant, and it cannot exceed the maximal value of v_{max}, fixed by adiabatic condition $v_{max} \ll \Omega$.

The parameters a, θ_M and $\Delta\phi$ are connected by the relation $a = \Delta\phi(1 - \cos \theta_M)$. The error δ_{tr} is then

$$\delta_{tr} = \delta_{tr}^M + \delta_{tr}^P, \tag{20}$$

where

$$\delta_{tr}^M = \frac{K}{v}\left(\theta_M - \frac{1}{4}\sin 4\theta_M\right) \tag{21}$$

is the contribution along the meridian and

$$\delta_{tr}^P = K\frac{a}{v}\frac{\sin \theta_M \sin^2 2\theta_M}{1 - \cos \theta_M} \tag{22}$$

is the contribution along the parallel.

In Fig. 1 δ_{tr} is plotted for $a = \pi/2$ and $a = \pi/4$ (corresponding to NOT and Hadamard gate respectively) as a function of θ_M. One can see that δ_{tr} has a local minimum for $\theta_M = \pi/2$ and a global minimum for $\theta_M = 0$ where the error vanishes. This suggests that the best choice is to take θ_M as small as possible.

It is interesting to consider the dependence of δ_{tr} also on the evolution time t_{ad}. For simplicity, we set the velocity $v = v_{max}$. In this case, changing θ_M (and then $\Delta\phi$) corresponds to a change in the evolution time. We obtain

$$\theta_M = \arccos\left(1 - \frac{a}{2\pi m}\right), \tag{23}$$

where

$$m = \frac{1}{4\pi a}\left[(v_{max}t_{ad})^2 + a^2\right]. \tag{24}$$

Using these relations, δ_{tr}^M and δ_{tr}^P, given by (21)-(22) become functions of t_{ad}, v_{max} and a. Note that m measures the space covered along the parallel, in fact $\Delta\phi = 2\pi m$.
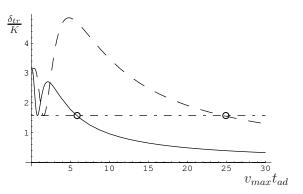

FIG. 2: The error δ_{tr} versus $v_{max}t_{ad}$ for two different a values: $a = \pi/2$ (dashed line) and $a = \pi/4$ (full line) correspond to NOT and Hadamard gate respectively. The dot-dashed line shows the value of the error at $\theta = \pi/2$. The circles show the critical value of $v_{max}t_{ad}$ above which the best loop is the one with the minimal θ_M.

In Fig. 2 we see the behavior of δ_{tr} as a function of $v_{max}t_{ad}$. The first minimum for both curves corresponds to $\theta_M = \pi/2$, then the curves for long t_{ad} decrease asymptotically to zero corresponding to the region in which $\theta_M \to 0$. In this regime we have $\delta_{tr} \propto 1/t_{ad}$ which is drastically different from the results obtained with other methods where $\delta_{tr} \propto t_{ad}$ (see Refs [4, 24] and below Section III C). It should be observed that this surprising results is a merit of holonomic approach which allows to choose the loop in the parameter space, without changing the logical operation as long as it subtends the same solid angle. Observe that small θ_M and long t_{ad} mean large value of m, i.e. multiple loops around the north pole.

Fig. 2 shows that, for a given gate, there is a critical value k_c of $v_{max}t_{ad}$ which discriminate between the choice of θ_M (e.g. $k = 6$ for the Hadamard gate and $k = 25$ for the NOT gate). For $v_{max}t_{ad} < k_c$ the best choice for the loop is $\theta_M = \pi/2$; For $v_{max}t_{ad} > k_c$ the best choice is the value of θ_M determined by equations (23) and (24).

Note that the region $v_{max}t_{ad} > k_c$ is accessible with physical realistic parameters [12]. For example, if we choose the laser intensity $\Omega = 20$meV and $v_{max} = \Omega/50$ (for which values the non-adiabatic transitions are forbidden), at the critical parameter corresponds critical time of 15 ps for the Hadamard gate and 42 ps for the NOT gate.

B. Pure Dephasing

Until now we have ignored the pure dephasing effect because we have assumed that it is negligible in comparison with the transition error for long evolution time. Now, we check that the pure dephasing error contribution can indeed be neglected. We can write the pure dephasing error using the Eq. (17) and splitting to parallel and

meridian part as

$$\delta_{pd}^P = \int_0^{t_{ad}} dt \int_0^\infty d\omega \frac{J(\omega)}{\omega} \coth(\frac{\omega}{2T})$$
$$Q(a(t)) \sin \omega t \sin^4 \theta_M \qquad (25)$$

and

$$\delta_{pd}^M = \int_0^{\frac{\theta_M}{v_{max}}} dt \int_0^\infty d\omega \frac{J(\omega)}{\omega} \coth(\frac{\omega}{2T}) Q(a(t))$$
$$\sin \omega t (\sin^4(v_{max}t) + \sin^4[\theta_M(1 - \frac{v_{max}t}{\theta_M})]) \qquad (26)$$

where $Q(a(t)) = 1 + 1/2 \sin^2(2a(t))$.

To estimate δ_{pd} we assume that t_{ad} is longer with respect to the characteristic time of bath. Remembering that $J(\omega) \propto \omega^s$, the pure dephasing error behavior along the parallel at the temperature T is

$$\delta_{pd}^P \propto \begin{cases} \left(\frac{1}{t_{ad}}\right)^{s+3}, & T \ll 1/t_{ad} \\ T \left(\frac{1}{t_{ad}}\right)^{s+2}, & T \gg 1/t_{ad} \end{cases} \qquad (27)$$

while along meridian is

$$\delta_{pd}^M \propto \left(\frac{1}{t_{ad}}\right)^3. \qquad (28)$$

Then, we can conclude that the pure dephasing can always be neglect for long time evolution because it decreases faster than the transition error.

C. Comparison between HQC and STIRAP

We make a comparison between Holonomic Quantum Computation (HQC) and the STIRAP procedure which is an analogous approach to process quantum information. The STIRAP procedure ([2, 4]) is, in its basic points, very similar to the holonomic information manipulation. The level spectrum, the information encoding, the evolution produced by adiabatic evolving laser are exactly the same. The fundamental difference is that in STIRAP the dynamical evolution is fixed (we must pass through precise sequence of states) and then the corresponding loop in the parameter space is fixed. In particular, we go from the north pole to the south pole and back to the north pole along meridians. Since the loop, as in our model, is a sequence of meridian-parallel-meridian path, we can calculate the error and make a direct comparison. In this case, the transition error results proportional to $\delta_{tr} \propto t_{ad}$ and grows linearly in time while for HQC $\delta_{tr} \propto 1/t_{ad}$. Therefore, the HQC is fundamentally favorite for long application time respect to the STIRAP ones.

Moreover, we can show that the freedom in the choice of the loop allows us to construct HQC which perform better than the best STIRAP gates. In Ref. [4] the minimum error (not depending on the evolution time) for STIRAP was obtained reaching a compromise between the necessity to minimize the transition, pure dephasing error and the constraint of adiabatic evolution. With realistic physical parameters [20] ($J(\omega) = k\omega^3 e^{(-\omega/\omega_c)^2}$, $\Omega = 10$ meV, $\epsilon = 1$eV, $v_{max} = \Omega/50$, $k = 10^{-2}$(meV)$^{-2}$, $\omega_c = 0.5$ meV and for low temperature), the total minimum error in Ref. [4] is $\delta(stirap) = 10^{-3}$. With the same parameters, we still have the possibility to increase the evolution time in order to reduce the environmental error. However, for evolution time $t_{ad} = 50$ps we obtain a total error $\delta = 1.5 \ 10^{-4}$ for the NOT gate and $\delta = 4 \cdot 10^{-5}$ for the Hadamard gate respectively. As can be seen, the logical gate performance is greatly increased.

D. More general noise

Until now we have discussed the possibility to minimize the environmental error by choosing a particular loop in the parameter sphere but the structure of the error functional clearly depends on the system-environment interaction. Then one might wonder if the same approach can be used for a different noise environment.

For this reason, we now briefly analyze the case of noise matrix in the form $A = diag\{0, 1, 0, -1\}$. Again, for long evolution we can neglect the contribution of the pure dephasing and focus on the transition error. In this case the interesting part of the error functional takes the form

$$\delta_{tr} = K[(\frac{1}{2} \sin 2\theta \cos 2\theta)^2 + (\sin \theta \sin 2\phi)^2]. \qquad (29)$$

Even if the analysis in this case is much more complicated, it can be seen that δ_{tr} has an absolute minimum for $\theta_M = 0$. The long time behavior is the same ($\delta_{tr} \propto 1/t_{ad}$) such that the results are qualitatively analogous to the above ones: for small θ_M loops (or long evolution at fixed velocity) the holonomic quantum gate present a decreasing error. Then even in this case it is possible to minimize the environmental error.

IV. CONCLUSIONS

In summary, we have analyzed the performance of holonomic quantum gates in presence of environmental noise focusing on the possibility to have small errors choosing different loops in the parameter manifold. Due to the geometric dependence, we can implement the same logical gate with different loops. Since different loops correspond to different dynamical evolutions, we have used this freedom to construct an evolution through "protected" or "weakly influenced" states leading to good holonomic quantum gates performances. Once fixed the physical parameters, this allows us to to establish which is the best loop in order to minimize the environmental

effect. We have shown that for long time evolutions the noise decreases as $1/t_{ad}$ while in the other cases it increases linearly with adiabatic time. We also have shown that the same features can be found with different kinds of noise suggesting the possibility to find a way to minimize the environmental effect in presence of any noise. These results open new possibility for implementation of holonomic quantum gates to build quantum computation because they seem robust against both control error and environmental noise.

APPENDIX A: MINIMIZING THEOREM

Let's consider the family $\mathcal{C}_n$ composed the closed curves generated by a sequence of n paths along a *parallel* ($\theta = const$) alternated with paths along a *meridian* ($\phi = const$). We call C_n a generic curve in this family. For example, the family $\mathcal{C}_1$ contains all the closed curves composed by the sequence of path *meridian-parallel-meridian* while the family $\mathcal{C}_2$ contains the curves *meridian-parallel-meridian-parallel-meridian*.

We argue that the closed curve minimizing the error in Eq. (18) can be found in the $\mathcal{C}_1$ family. First, we show that any closed curve in $\mathcal{C}_2$ spanning a solid angle a on the sphere can be replaced by a closed curve in $\mathcal{C}_1$ spanning the same angle and producing a smaller error. In analogous way any closed curve in $\mathcal{C}_3$ can be replaced by a closed curve in $\mathcal{C}_2$ with smaller error and so on. By induction we obtain that any closed curve in $\mathcal{C}_n$ can be replaced by a curve in $\mathcal{C}_1$ spanning the same solid angle but producing smaller error. Since the curve belonging to $\mathcal{C}_n$ can approximate any closed curve on the sphere, the best curve can be found in $\mathcal{C}_1$.

The crucial point is to show that any curve in $\mathcal{C}_2$ can be replaced by a curve in $\mathcal{C}_1$. Let's consider a generic curve C_2 in $\mathcal{C}_2$ spanning a solid angle a: composed by a segment of a *meridian* (with θ going from 0 to θ_1), a *parallel* (spanning a $\Delta\phi_1$ angle), a *meridian* (with $\theta : \theta_1 \to \theta_2$), a *parallel* (spanning a $\Delta\phi_2$ angle), and finally a segment to the *north pole* along a *meridian*. Let's consider two closed curves C_1^1 and C_1^2 in $\mathcal{C}_1$ subtending the same solid angle a with, respectively, θ_1 and θ_2 as maximum angle spanned during the evolution along the *meridian*. First we analyze (20) along the *meridian*. Without loosing generality, we can take $\theta_1 < \theta_2$; it is clear from Eq. (21) that the value of δ_{tr} along the *meridian* for C_1^1 is smaller that for C_1^2: $\delta_{C_1^1}^M < \delta_{C_1^2}^M$. We note from the Eq. (21), suitable extended to C_2, that the two paths along the *meridians* depends only on θ_2 and then produce the same error of C_1^2,

$$\delta_{C_1^1}^M < \delta_{C_1^2}^M = \delta_{C_2}^M. \tag{A1}$$

The difference between the contribution along the *parallel* is

$$\delta_{C_2}^P - \delta_{C_1^2}^P = \Delta\phi_1\left(\sin\theta_1\sin^2 2\theta_1 - \frac{1-\cos\theta_1}{1-\cos\theta_2}\sin\theta_2\sin^2 2\theta_2\right) \tag{A2}$$

and

$$\delta_{C_2}^P - \delta_{C_1^1}^P = \Delta\phi_2\left(\sin\theta_2\sin^2 2\theta_2 - \frac{1-\cos\theta_2}{1-\cos\theta_1}\sin\theta_1\sin^2 2\theta_1\right) \tag{A3}$$

Analysis of the positivity of the quantities given by Eq. (A2) and (A3) shows that $\delta_{C_2}^P$ cannot be at the same time smaller than $\delta_{C_1^1}^P$ and $\delta_{C_1^2}^P$. In fact, there are two possibilities: If $\delta_{C_2}^P > \delta_{C_1^1}^P$, from Eq. (A1) and (A3)

$$\delta_{C_2} = \delta_{C_2}^M + \delta_{C_2}^P > \delta_{C_1^1}^M + \delta_{C_1^1}^P = \delta_{C_1^1} \tag{A4}$$

and the best closed curve is C_1^1. If $\delta_{C_2}^P > \delta_{C_1^2}^P$, from Eq. (A1) and (A2)

$$\delta_{C_2} = \delta_{C_2}^M + \delta_{C_2}^P > \delta_{C_1^2}^M + \delta_{C_1^2}^P = \delta_{C_1^2} \tag{A5}$$

and the best closed curve is C_1^2.

In same way it can be show that any closed curve in $\mathcal{C}_3$ can be replaced by a closed curve in $\mathcal{C}_2$ with smaller error.

[1] P. Zanardi and M. Rasetti, Phys. Lett. A **264**, 94 (1999).
[2] Z. Kis and F. Renzoni, Phys. Rev. A **65**, 032318 (2002).
[3] F. Troiani, E. Molinari and, U. Hohenester, Phys. Rev. Lett. **90**, 206802 (2003).
[4] K. Roszak, A. Grodecka, P. Machnikowski, and T. Kuhn, Phys. Rev. B **71**, 195333 (2005).
[5] J. A. Jones, V. Vedral, A. Ekert, and G. Castagnoli, Nature (London) **403**, 869 (2000).
[6] G. Falci, R. Fazio, G. M. Palma, J. Siewert, V. Vedral, Nature (London) **407**, 355 (2000).
[7] R. G. Unanyan, B.W. Shore, and K. Bergmann, Phys. Rev. A **59**, 2910 (1999).
[8] L.-M. Duan, J.I. Cirac, and P. Zoller, Science **292**, 1695 (2001).
[9] L. Faoro, J. Siewert, and R. Fazio, Phys. Rev. Lett. **90**, 028301 (2003).
[10] I. Fuentes-Guridi, J. Pachos, S. Bose, V. Vedral, and S. Choi, Phys. Rev. A **66**, 022102 (2002).

[11] A. Recati, T. Calarco, P. Zanardi, J. I. Cirac, and P. Zoller, Phys. Rev. A **66**, 032309 (2002).

[12] P. Solinas, P. Zanardi, N. Zanghì, and F. Rossi, Phys. Rev. B **67**, 121307(R) (2003).

[13] A. Carollo, I. Fuentes-Guridi, M. F. Santos, and V. Vedral, Phys. Rev. Lett. **90**, 160402 (2003).

[14] G. De Chiara and G. M. Palma, Phys. Rev. Lett. **91**, 090404 (2003).

[15] A. Carollo, I. Fuentes-Guridi, M. F. Santos, and V. Vedral, Phys. Rev. Lett. **92**, 020402 (2004).

[16] V.I. Kuvshinov and A.V. Kuzmin, Phys. Lett. A, **316**, 391 (2003).

[17] P. Solinas, P. Zanardi, and N. Zanghì, Phys. Rev. A 70, 042316 (2004).

[18] S.-L. Zhu and P. Zanardi, Phys. Rev. A **72**, 020301(R) (2005).

[19] G. Florio, P. Facchi, R. Fazio, V. Giovannetti and S. Pascazio, Phys. Rev. A **73**, 022327 (2006);

[20] D. Parodi, M. Sassetti, P. Solinas, P. Zanardi, and N. Zanghì, Phys. Rev. A **73**, 052304 (2006).

[21] The explicit expression for the *bright* states is $|E_1\rangle = \frac{1}{\sqrt{2}\Omega}(\Omega|e\rangle + \sum_i \Omega_i|i\rangle)$ and $|E_2\rangle = \frac{1}{\sqrt{2}\Omega}(-\Omega|e\rangle + \sum_i \Omega_i|i\rangle)$; for the *dark* states is $|E_3\rangle = 1/(\Omega\sqrt{|\Omega_+|^2 + |\Omega_-|^2})[\Omega_0(\Omega_+|+\rangle + \Omega_-|-\rangle) - (\Omega^2 - |\Omega_0|^2)|0\rangle])$ and $|E_4\rangle = 1/\sqrt{|\Omega_+|^2 + |\Omega_-|^2}[\Omega_-|+\rangle - \Omega_+|-\rangle]$

[22] A. O. Caldeira and A. J. Leggett, Phys. Rev. Lett. **46**, 211 (1981).

[23] U. Weiss, *Quantum dissipative systems* (World Scientific, Singapore, 1999).

[24] R. Alicki, M. Horodecki, P. Horodecki, R. Horodecki, L. Jacak, and P. Machnikowski, Phys. Rev. A **70**, 010501(R) (2004).